

Craniosynostosis in the Middle Pleistocene human Cranium 14 from the Sima de los Huesos, Atapuerca, Spain

Ana Gracia^{a,1}, Juan Luis Arsuaga^{a,b,1}, Ignacio Martínez^{a,c}, Carlos Lorenzo^d, José Miguel Carretero^e, José María Bermúdez de Castro^f, and Eudald Carbonell^d

^aCentro Mixto UCM-ISCIH de Evolución y Comportamiento Humanos, ^cSinesio Delgado 4, Pabellón 14, 28029 Madrid, Spain; ^bDepartamento de Paleontología, Facultad de Ciencias Geológicas, Universidad Complutense de Madrid, 28040 Madrid, Spain; ^dÁrea de Paleontología, Departamento de Geología, Universidad de Alcalá de Henares, 28871 Alcalá de Henares, Spain; ^eInstitut de Paleoeologia Humana i Evolució Social-Area de Prehistoria, Facultat de Lletres, Universitat Rovira i Virgili, Plaça Imperial Tàrraco 1, 43005 Tarragona, Spain; ^fDepartamento de Ciencias Históricas y Geografía, Facultad de Humanidades y Educación, Universidad de Burgos, 09001 Burgos, Spain; and ¹Centro Nacional de Investigación sobre la Evolución Humana, Avenida de la Paz 28, 09004 Burgos, Spain

Contributed by Juan Luis Arsuaga, February 12, 2009 (sent for review October 7, 2008)

We report here a previously undescribed human Middle Pleistocene immature specimen, Cranium 14, recovered at the Sima de los Huesos (SH) site (Atapuerca, Spain), that constitutes the oldest evidence in human evolution of a very rare pathology in our own species, lambdoid single suture craniosynostosis (SSC). Both the ecto- and endo-cranial deformities observed in this specimen are severe. All of the evidence points out that this severity implies that the SSC occurred before birth, and that facial asymmetries, as well as motor/cognitive disorders, were likely to be associated with this condition. The analysis of the present etiological data of this specimen lead us to consider that Cranium 14 is a case of isolated SSC, probably of traumatic origin. The existence of this pathological individual among the SH sample represents also a fact to take into account when referring to sociobiological behavior in Middle Pleistocene humans.

human evolution | paleopathology | sociobiology | congenital skull deformation

Paleopathology is the study of past diseases. In paleoanthropology, this is generally restricted to lesions of the bones and teeth. However, paleopathology can also inform about past human behavior in healthy individuals (ref. 1 and references therein), being cautious with the interpretation of health status of individuals and population based on any paleontological data (2, 3). Some pathological lesions produced by or related to human activities, including dietary aspects, can be treated, and social support can be provided by relatives or other members of the social group. Also, it is possible to hypothesize whether an affected individual would have been able to keep up with the group and provide for themselves within a hunter gatherer context, or whether long term survival due to a serious illness or injury was impossible without assistance from other members of the social group. Neanderthals as well as other Pleistocene hominins have been claimed by some authors to likely have shown social caring for ill/nonautonomous individuals, in the same way as only modern humans have (1, 4). Here, we discuss a Middle Pleistocene case of a serious congenital skull deformation that may have required extra conspecific care for the individual to survive for a number of years before he/she died at the end of childhood.

Description of Cranium 14

The new Cranium 14 (Figs. 1 and 2) is part of a hominin sample of at least 28 individuals of a European Middle Pleistocene *Homo* population that are being unearthed at the Sima de los Huesos (SH) site (Atapuerca, Spain) since 1976 (5, 6). The most recent attempts to date the site have provided a firm minimum age of 530 kya for the fossil human assemblage (7).

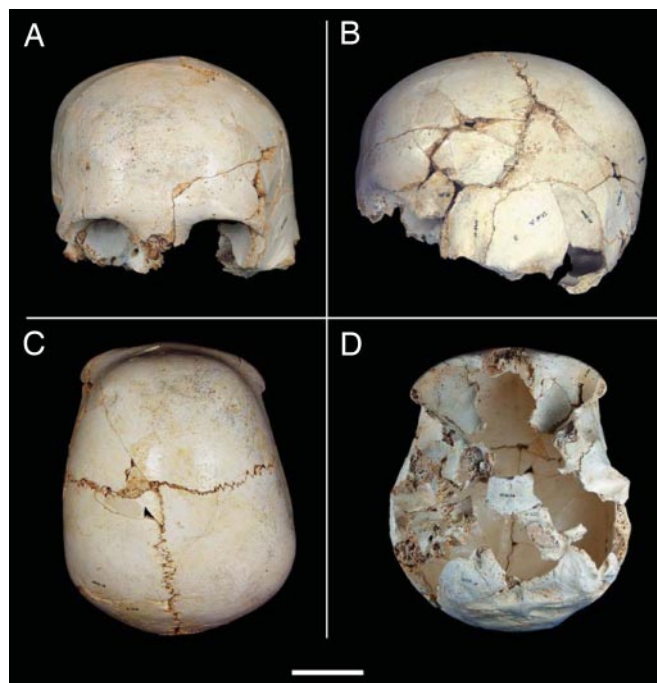


Fig. 1. Cranium 14 from SH site. (A) Frontal view, showing the left glenoid and mastoid regions well below those of the right side. (B) Left lateral view. Note the rounded profile, and the vertical forehead. (C) Superior view. The projection of the torus supraorbitalis can be clearly seen. (D) Inferior view, revealing the characteristic deformities of this craniosynostosis: The posterior part of the cranium is twisted to the left with respect to the sagittal plane; the left glenoid cavity is more anteriorly placed than the right one. (Scale bar, to 5 cm.)

The new cranium was recovered in many pieces during the 2001 and 2002 field seasons [Fig. S1 *A* and *B* and Movie S1; for fragments and labels, see *Materials and Methods*], and has been reconstructed during the subsequent years. As it happens with

Author contributions: A.G. designed research; A.G., I.M., C.L., and J.L.A. performed research; A.G., J.L.A., I.M., C.L., J.M.C., J.M.B.d.C., and E.C. contributed new reagents/analytic tools; A.G. and J.L.A. analyzed data; and A.G., J.L.A., and I.M. wrote the paper.

The authors declare no conflict of interest.

See Commentary on page 6429.

¹To whom correspondence may be addressed. E-mail: agracia@isciii.es or jlarsuaga@isciii.es.

This article contains supporting information online at www.pnas.org/cgi/content/full/0900965106/DCSupplemental.

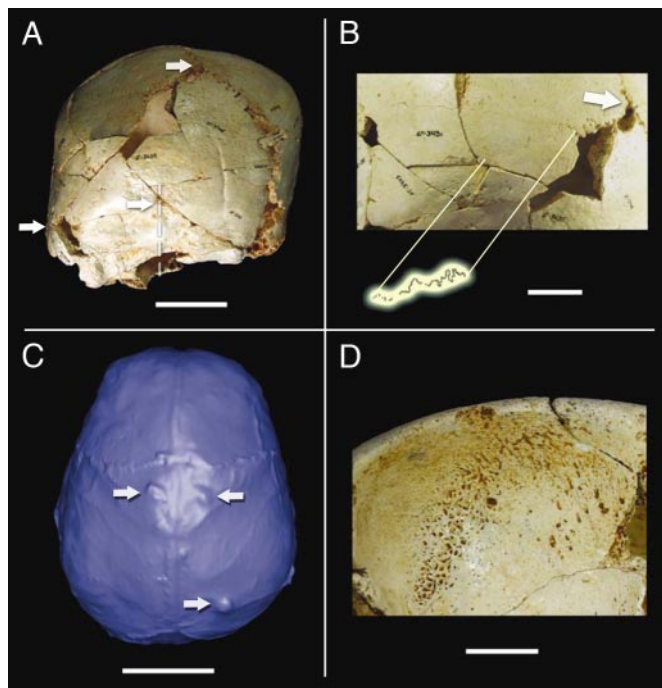


Fig. 2. Relevant features in Cranium 14. (A) Posterior view, showing the parallelogram profile and the ipsilateral occipito-mastoid bulge, both diagnostic features of the left lambdoid suture premature fusion. Note the deviation of the sagittal plane with respect to the sagittal suture plane, showing that the Inion, the occipital crest and other medial structures of the nuchal plane are positioned 10 mm or more to the left. From top to bottom, the white arrows mark the craniometric points Lambda, Inion, and left Asterion, respectively. Discontinuous lines show the displacement of the sagittal suture and the occipital midline. (Scale bar, 5 cm.) (B) Close-up of part of the left lambdoid synostosis. The section where the suture is almost completely obliterated is enhanced above. (Scale bar, 2 cm.) (C) Virtual endocast of Cranium 14, superior view. Upper arrows point to the bregmatic arachnoid granulations. Lower arrow points to the obelionic arachnoid granulation. (Scale bar, 5 cm.) (D) Cribra orbitalia on Cranium 14 right orbital roof. (Scale bar, 1 cm.)

the other fossils from this site, the pieces show different degrees of breakage, but are in very good state of preservation, allowing accurate reconstructions, for example, see Cranium 5 (6). It is especially important to point out that no postmortem deformation has been found in either this particular specimen, nor in any other fossils of this collection (8).

Cranium 14 consists of an almost complete neurocranium lacking the face, the petrous and mastoid processes of the left temporal bone, the right occipital condyle, the ethmoid bone, and the central part of the sphenoid bone. After reconstruction, Cranium 14 revealed a premature suture fusion between the left parietal and occipital bones (Fig. 2A and B; Fig. S2), which is the core of the present study.

Age at Death

Cranium 14 belonged to an immature individual. There are two completely open syncondroses preserved: the spheno-occipital (Fig. S3) and the jugular (both sides). The occipital surface of the spheno-occipital one shows the characteristic immature irregular and rugous pattern of unfused syncondrosis, without any bridging even in the endocranial border (9). The time of closure of the spheno-occipital syncondrosis among modern human populations is variable, ranging from the extreme cases that started at ≈ 11 - to 13- up to 18-years-old, depending on the reference sample/author (9, 10).

Although the closing time of the jugular syncondrosis is even more variable (9, 11), its lower limit is well inside the range of

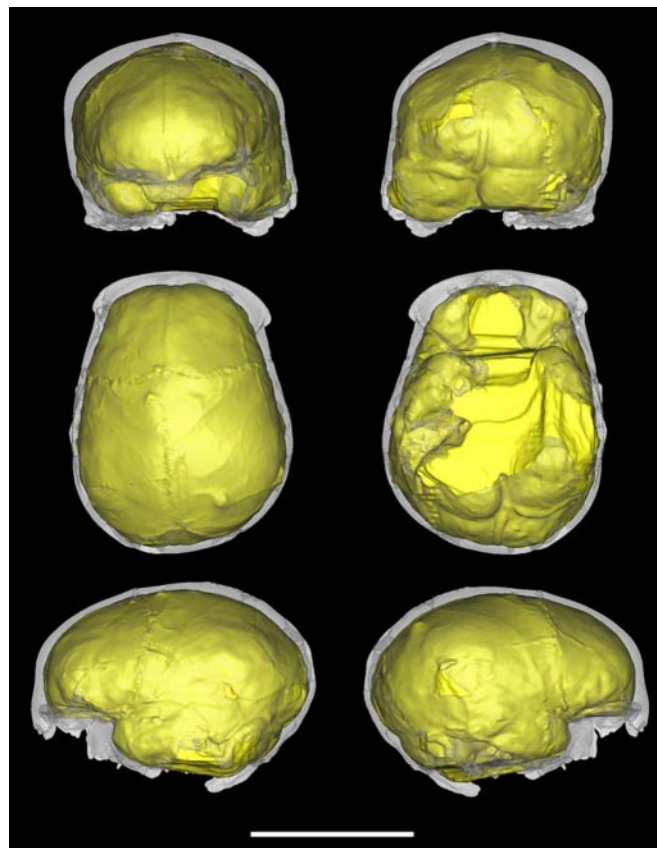


Fig. 3. Virtual endocast of Cranium 14. From top to bottom, left to right: frontal, posterior, superior, inferior, left lateral, and right lateral views. Note the general bilateral asymmetry, the occipitomastoid bulging of the left side, the anteriorly placed left temporal lobe compared with the right, and the protruding left occipital pole. (Scale bar, 10 cm.)

the spheno-occipital syncondrosis, and appears always fused in all of the SH adult specimens (12). Thus, based on these two syncondroses, Cranium 14 had not reached adulthood in any case, and its age at death was well < 18 -years-old.

However, the 3D CT scan reconstructions of the specimen (Fig. 2C and Fig. 3; for virtual reconstruction, see *Materials and Methods*), have allowed us to estimate its endocranial volume at $\approx 1,200$ cm³. This value is within the SH adult range of variation (Cranium 5 is $\approx 1,100$ cm³ and Cranium 4 is 1,390 cm³), and it is nearly identical to that estimated for the 13.5-years-old Cranium 6 (6, 13). If brain development of SH hominids is similar to that of modern humans, as it has been suggested in some studies (14–16), the individual represented by Cranium 14 was at least 5- to 8-years-old, because it had reached an adult brain size by the time he/she died.

Last, we have observed that the torus supraorbitalis is much more gracile in immature specimens of the SH sample than it is in adult individuals (6). The most important age-related thickness differences in the supraorbital torus are found at the medial point (TMOP) and the lateral point (TLP). To try a more accurate estimation of the age at death of Cranium 14, we have compared its torus supraorbitalis thickness to other two immature specimens that have associated dentitions, both with an estimated age at death ranging from 12.5- to 14.5-years-old (6, 17, 18): Cranium 6, which corresponds to SH dental individual XX, and Cranium 9, whose left frontal fragment AT-626 was published earlier (6), and now has been associated to SH dental individual XVI.

Table 1. Supraorbital thickness of some SH specimens

| | SH individuals no. | Age at death, y | Supraorbital thickness | | Source |
|-----------------------------|--------------------|-----------------|------------------------|------|---------------------|
| | | | TLP | TMOP | |
| <i>Immature individuals</i> | | | | | |
| Cranium 6 | XX | 12.5–14.5 | 8 | 7.4 | Authors, ref. 6 |
| Cranium 9 | XVI | 12.5–14.5 | 6.5 | 6.8 | Authors, ref. 6 |
| Cranium 14 | — | 5–12.5 | 5 | 4 | Authors, this study |
| <i>Adult individuals</i> | | | | | |
| Cranium 4 | — | Adult | 12.0 | 11.5 | Authors, ref. 6 |
| Cranium 5 | XXI | >35 | 14.6 | 14.1 | Authors, ref. 6 |

SH individual no. is from refs. 17 and 18. Although Cranium 4 does not have associated dentition, it is the oldest specimen of the SH sample using age-cranial suture closure assessment. TLP, thickness at the lateral point; TMOP, thickness at the midorbital point; y, years old.

Cranium 14 supraorbital thickness values at TMOP and TLP are well below those of Cranium 6 and Cranium 9 (Table 1); thus, its age at death should have been lower than that of those individuals.

After all these criteria, we conclude that the most probable age at death for Cranium 14 is somewhat below the lower limit estimated for Cranium 6 and Cranium 9 (i.e., <12.5-years-old), and, compared with the development of living populations (14, 15), older than 5- to 8-years-old.

Description of the Pathological Condition

Cranium 14 has almost complete fusion of the left lambdoid suture, except for the first ≈ 31 mm below the estimated Lambda (Fig. 2 *A* and *B*; Fig. S2). The total arc length of the right (nonfused) lambdoid suture (≈ 85 mm) is much shorter than the left side lambdoid arc length (≈ 114 mm). On the right lambdoid suture, there is, at least, one small wormian bone (Fig. 2*A*; Fig. S4*A*). Starting at the lowest nonfused left lambdoid suture end, a well-marked horizontal depression crosses from one lambdoid suture to the other at the occipital apex (Fig. 2*A*; Fig. S4*A*). In our opinion, it is a remainder of a complete fusion of the inferior suture of a triangular-shaped wormian bone. These triangular-shaped lambdoid wormian bones are frequent within the SH population (6, 19), but they never appear fused, not even in the older individuals (Fig. S4*B*).

In addition to the left unilateral lambdoid synostosis, Cranium 14 shows contralateral parietal bossing, a very conspicuous ipsilateral occipitomastoid bulge, and an ipsilateral inferior tilt of the skull base (Figs. 2*A* and 4; Fig. S5); also seen in the

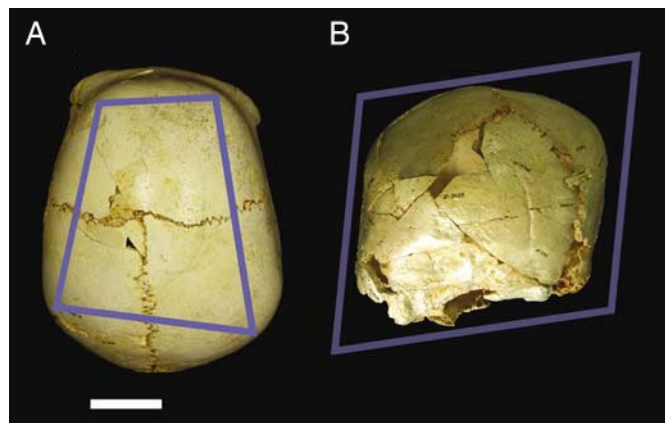


Fig. 4. Diagnostic profiles of unilambdoid synostosis of Cranium 14. (A) Trapezoid-shape in vertex view. (B) Parallelogram profile in posterior view. (Scale bar, 5 cm.)

reconstructed endocast (Fig. 3). The foramen magnum, the external occipital crest, the Inion, and the suprainiac area are off-set and twisted 8° to the left with respect to the plane of the sagittal suture (Figs. 1*D*, 2*A*, and 3). The relative positions of the glenoid cavities, which is an indirect measure of ear symmetry, is displaced with respect to both the foramen magnum, the sagittal suture plane and also a coronal plane (Figs. 1*A* and *D*, 2*A*, and 3; compare coronal slices 80/100 in Fig. S5). The left glenoid cavity is located 4.4 mm below and 10.1 mm anterior to that on the right side. The frontal bone morphology of all archaic *Homo* fossils (i.e., non-*Homo sapiens*) displays a receding frontal squama, and its maximum curvature is always located along the sagittal plane, whereas the modern human frontal squama is usually vertical, and the two frontal bosses are well defined. As in some cases of lambdoid single suture craniosynostosis (SSC) (20), Cranium 14 frontal squama presents a little right (contralateral) frontal projection. Also, Cranium 14 displays verticalization of the forehead and individualization of the two frontal bosses, which superficially makes this specimen resemble the condition seen in modern humans (Fig. 1*A* and *B*).

The endocranial surface of Cranium 14 presents strong asymmetries (Figs. 2*C* and 3; Fig. S5), particularly in the region of the temporal lobes, with the left side shorter and more anteriorly placed than the right side (Fig. 3; see slice 120 in Fig. S5). The endocranial convolutions are abnormally projected and much more deeply marked at the distal end of the occipital poles, at the endometopic region, at the left parietal tuber, and at the cerebellar poles. On the internal table of the frontal bone, perpendicular to the sulcus sagittalis, an anomalous and smooth capillary network is present. Three very broad and developed subarachnoid fossae are visible on the parietal bones (Fig. 2*C*). Two of them are more or less symmetrically placed at the end of the bregmatic branches of the middle meningeal system, and the third one, which is the largest and deepest of the three, is located on the obelionic region of the right parietal bone.

Differential Diagnosis and Possible Etiological Factors

Cranium 14 displays a premature lambdoid suture fusion, an uncommon pathology included among birth defects known as craniosynostosis (20, 21), specifically a type described as SSC (21–25). Most modern understanding of craniosynostosis is referenced from the 1851 writings of Virchow (26). Unilateral lambdoid synostosis is a rare pathology, occurring <6 in every 200,000 individuals in living humans (27, 28).

There is abundant literature about plagiocephalia in modern populations due to its interest regarding the sudden infant death syndrome (24, 21 and all references therein); thus, a lot of attention has been paid to make the differential diagnosis of plagiocephalia (deformational or positional plagiocephalia

versus a real unilateral lambdoidal synostosis (20–23, 29, 30)) in living children, because the treatment differs depending on it.

Cranium 14 displays a trapezoidal-shaped and parallelogram profiles in vertex and posterior views, respectively (Fig. 4 *A* and *B*), which are definitive diagnostic signs of unilateral lambdoidal synostosis in modern children (20–32), as well as the 8° of the off-set ipsilateral deviation of the intersection of posterior fossa axis and the anterior fossa axis (29). This deformation is the result of the premature fusion reaction that produces: “First, in true lambdoidal synostosis, the contralateral posterior bossing more laterally and superiorly, in the parietal region. Second, frontal bossing is not a striking feature, but when it occurred, it was contralateral rather than ipsilateral. (...) Third, ipsilateral occipitomastoid bossing was consistently present in lambdoidal synostosis, whereas it was conspicuously absent in deformational posterior plagiocephaly” (20). As it has been established for other craniosynostotic cases in modern populations, the misshapen cranial abnormalities present in Cranium 14 constitute a secondary response to the lambdoidal synostosis, rather than a causal factor (24). The same must be true for the presence of the small right lambdoidal ossicle (Fig. S4*A*). As has been documented for intentionally deformed modern human skulls (33), we consider the presence of small lambdoidal ossicles to be further evidence of an anomalous compensatory rapid growth that also produced the contralateral displacement of the right parietal tuber. Unlike many other synostotic cases (20), the fused suture is not ridged in this specimen. The same holds true for other lambdoidal synostosis studied in modern humans, where no significant ridging was found (34). The fusion seems to have been edge to edge, and the exocranial (Fig. 2*A*; Fig. S2) and endocranial surfaces of the synostosed suture appear continuous and smooth.

The parietal, temporal, and occipital deformations seen in this fossil are very similar to other “true” plagiocephalic cases (e.g., see figures 6 and 7 in ref. 22), and, with regard to the frontal bone morphology, in this case, the frontal squama compensatory deformation does not result in a conspicuous contralateral bossing, as it has sometimes been found in modern human populations (20–24). On the contrary, as described above, the compensatory distortion on the frontal bone of Cranium 14 resulted in a modern-like frontal bone morphology (Fig. 1*A* and *B*). The same holds true with respect to the glenoid cavity asymmetry, which more frequently presents a posterior position for the ipsilateral glenoid fossa, but, in other cases, it can be found anteriorly placed or even not displaced at all (21).

With regard to the etiology of SSC, it is very difficult to establish it, even for modern humans. Nevertheless, we have some arguments that can be applied to the case of Cranium 14 SSC.

The premature unilambdoidal fusion found in Cranium 14 can be the result of primary or secondary craniosynostosis, being defined the former as the “polar term of the pair” *sensu* Cohen (21), where “sutural obliteration is secondary to a known disorder.”

In a suture fused prematurely, growth is mainly restricted orthogonal to the fused suture, from the ossification center to the fused suture (34–36). Although growth does not completely stop, almost no change is seen during development. In response to a prematurely closed suture, the remaining sutures undergo compensatory growth in a very fixed pattern (35, 36). In Cranium 14, the primary ossification center (parietal protuberance) of the left parietal bone is very close in straight line (perpendicular) to the fused lambdoidal suture (arc, ≈30 mm; chord, ≈28 mm) (Fig. 2*A*; Fig. S2). According to this criteria, and assuming that the newborn parietal is square shaped (9) and that fetal development and newborn-brain size were similar to that of modern humans (15, 16), the distance in Cranium 14 would correspond to a modern *H. sapiens* fetal parietal bone with a maximum width of ≈60 mm, size that is reached between 28

and 34 fetal weeks (9). These data suggest that the synostosis of this suture in Cranium 14 was initiated during the third term of fetal development.

Thus, considering that there is some evidence about the timing of the initiation of the fusion, the possible etiology of the SSC of Cranium 14 can be summarized as follows. The first case would be premature SC of traumatic origin due either to (*i*) intrauterine stress/constraint (37), (*ii*) torticollis congenita (21, 38), or (*iii*) intrauterine trauma (21) and would exclude other frequently quoted, labor complications (39, 40). The second case would be premature SC due to a metabolic disease, either (*i*) rickets and/or (*ii*) anemia. Cranium 14 also shows the most pronounced example of cribra orbitalia (Fig. 2*D*) within the entire SH sample (compare with ref. 41). The right orbit is severely affected, showing extensive pitting on the roof. Both anemia and rickets are claimed to be metabolic causes associated with the presence of cribra orbitalia (42, 43). Since rickets and anemia have been related to some cases of craniosynostosis (34, 44, 45), we cannot exclude these metabolic diseases as the possible trigger factor of the premature suture fusion. Nevertheless, we consider these options less probable, because except for some genetic vitamin D deficiencies, these pathological conditions develop after birth, and in Cranium 14, the synostosis seems to have started during the fetal stage. Also, in Cranium 14 there are no other cranial signs usually associated to rickets or anemia, such as porotic hyperostosis.

Discussion

There are some references about pathological specimens from the Pleistocene hominid fossil record with serious developmental/degenerative abnormalities. Among them, the oldest is dated in 1.77 kya and corresponds to that of the edentulous D3444/D3900 individual from the Dmanisi site, who “apparently survived for a lengthy period without consuming foods that required heavy chewing” (46). In this study, the survival of this specimen was interpreted as a possible evidence of conspecific care. Another case of some degree of survival after an important disorder is that of the individual represented by the Hulu 1 cranium, that presents signs of a healed pathological lesion on the neurocranial vault surface (1). With respect to malformations, there are two cases of special interest: the cranium of Salé, whose occipital deformation was interpreted as a result of torticollis congenita (47), and the temporal bone pathology from Singa 1, which lacks the structures of the bony labyrinth (48). This Middle Pleistocene specimen also presents parietal diploic expansion, and was previously cited as a probable case of premature synostosis of the sagittal suture (49). In our opinion, premature sagittal synostosis was not present in the Singa 1 specimen, because, in almost all sagittal synostosis cases, the vertex cranial shape should be elongated antero-posteriorly (scaphocephalia) and, in posterior view, with a disproportionately narrow cranium (27), which is not the case of this specimen.

As it has been claimed by DeGusta (50), inferences made about behavior in fossil hominid populations from skeletal pathologies must be tested with a comparative approach, but it is clear that the fossil evidence of individual cases that survived with different degrees of impairment has increased a lot (1 and references therein), and have been pointed out in some cases as evidence of conspecific care (4, 46).

The present pathology of Cranium 14 from the SH site must also be considered from this point of view, due to the handicapping lesions that this individual could have had. It is obvious that the SH hominid species did not act against the abnormal/ill individuals during the infancy, as has happened along our own history many times and in many cultures, and can be illustrated, for example, with the case of the elevated frequency of craniosynostosis found in the cemetery of the Medieval Hospital of St. James and St. Mary Magdalene (Chichester, England), that worked as an almshouse since AD 1450, where children with

deforming congenital conditions among others were abandoned (51).

The premature sutural synostosis, as well as the abnormal endocranial features found in Cranium 14, especially the presence of dilatation of subarachnoid spaces, were probably associated with an elevated intracranial pressure, as it has been described for SSC cases in living humans (24, 28, 31, 32, 52, 53). Most cases of craniosynostosis, both of genetic or epigenetic origin (syndromes, torticollis congenita, genetic or metabolic diseases, intrauterine position stress, traumas, labor complications; see refs. 21, 24, 31–41), are normally present before birth, and are noticeable externally during the first year of life. Also, genetic and severe nongenetic cases worsen during growth, including both the cognitive capabilities and the aesthetics of the individual (21, 22, 24, 25, 27, 30–32, 45). And finally and probably most importantly, there are known cases of premature SSC associated with a variable degree of mental retardation and/or elevated intracranial pressure (20–26, 31, 52–58).

Despite the severe pathological signs present in Cranium-14 child already described, it is not possible to estimate the degree of mental retardation.

In conclusion, Cranium 14 is the earliest documented case of craniosynostosis with resulting neurocranial, brain deformities, and, very likely, asymmetries of the facial skeleton. Despite these handicaps, this individual survived for >5 years, suggesting that her/his pathological condition was not an impediment to receive the same attention as any other Middle Pleistocene *Homo* child.

Materials and Methods

Cranium 14. Cranium 14 is composed of the following labeled fragments: AT-2044, AT-3239, AT-3400, AT-3403, AT-3405, AT-3406, AT-3411, AT-3412,

AT-3413, AT-3416, AT-3430, AT-3431, AT-3432, AT-3434, AT-3435, AT-3436, AT-3439, AT-3442, AT-3451, AT-3893, AT-3896, AT-3898, AT-4234, AT-4236, AT-6224, and AT-6225.

Virtual Reconstruction of Cranium 14 and Its Endocranium. CT image data of Cranium 14 was scanned with a YXLON Compact (YXLON International X-Ray) industrial multislice computed tomography (CT) scanner, located in Burgos University, Spain. The specimen was aligned along a cranial-caudal axis with the browridge facing upwards, to obtain *para*-coronal slices. Scanning parameters were: scanner energy 160 kV and 4 mA. Slice thickness was collimated to 0.5 mm, interslice spacing was 0.5 mm, and field of view 299.47 mm, reconstruction interval of 0.5 mm; 390 slices were obtained as a 1,024 × 1,024 matrix of 32-bit Float format with a pixel size of 0.216 mm, and transferred for processing. By using commercially available software package Mimics v.10.0, (Materialise), the CT image data of Cranium 14 were visualized, studied, measured, and processed to make a virtual endocast. The internal braincase was enclosed manually to close any contour gaps in the skullcap, and to “complete” any missing areas in Cranium 14 to the minimum surface. The virtual 3D endocast was created with a cavity fill operation within the Mimics 3D Segmentation module. The estimated encephalic volume, which is a minimum value, is 1,200 cm³. This value is the same as that obtained for Cranium 6, which was recalculated in a previous study, yielding an estimation of 1,200 cm³ (59).

ACKNOWLEDGMENTS. We thank the Atapuerca excavation team, especially that of the Sima de los Huesos; the Burgos University for providing the CT scanner; L. Rodríguez, E. Santos, and R. García for their technical assistance in CT scanning; Y. Rak, W. Hylander, A. Bartsiokas, R. Quam, G. Cuenca-Bescós, M. Martín-Loeches, and the 2 reviewers, who provided helpful comments; A. Bonmatí, F. Gracia, J. Lira, and J. Trueba (Madrid Scientific Films) for their help with the figures, photographs, and video; and Kennis & Kennis for their portrait of Cranium 14. This work was supported by Ministerio de Ciencia y Tecnología Spanish Government Grant CGL2006-13532-C03-02. The field excavation work was supported by Junta de Castilla y León and Fundación Atapuerca.

- Shang H, Trinkaus E (2008) An ectocranial lesion on the Middle Pleistocene human cranium from Hulu cave, Nanjing, China. *Am J Phys Anthropol* 135:431–437.
- Wood JW, Milner GR, Harpending HC, Weiss KM (1992) The Osteological Paradox: Problems of Inferring Prehistoric Health from Skeletal Samples. *Curr Anthropol* 33:343–370.
- Brothwell DR (1981) *Digging up Bones: The Excavation, Treatment and Study of Human Skeletal Remains*, British Museum of Natural History (Oxford Univ Press, Oxford), pp 1–208.
- Lebel S, Trinkaus E (2002) Middle Pleistocene human remains from the Bau de l'Aubesier. *J Hum Evol* 43:659–685.
- Arsuaga JL, et al. (1997) Sima de los Huesos (Sierra de Atapuerca, Spain). The site. *J Hum Evol* 33:109–127.
- Arsuaga JL, Martínez I, Gracia A, Lorenzo C (1997) The Sima de los Huesos crania (Sierra de Atapuerca, Spain). A comparative study. *J Hum Evol* 33:219–281.
- Bischoff JL, et al. (2007) High-resolution U-series dates from the Sima de los Huesos hominids yields 600 kyrs: Implications for the evolution of the early Neanderthal lineage. *J Archaeol Sci* 34:763–770.
- Arsuaga JL, Carretero JM, Gracia A, Martínez I (1990) Taphonomical analysis of the human remains from the Sima de los Huesos Middle Pleistocene site (Atapuerca/beas, Spain). *Hum Evol* 5:505–513.
- Scheuer L, Black S, eds (2000) *Developmental Juvenile Osteology*, eds Scheuer L, Black S, (Academic, London), pp 36–170.
- Bonmatí A, Arsuaga JL, Lorenzo C (2008) Revisiting the Developmental Stage and Age-at-Death of the “Mrs. Ples” (Sts 5) and Sts 14 Specimens from Sterkfontein (South Africa): Do They Belong to the Same Individual? *Anat Rec* 291:1707–1722.
- Hershkovitz I, et al. (1997) The elusive petrooccipital articulation. *Am J Phys Anthropol* 103:365–373.
- Martínez I, Arsuaga JL (1997) The temporal bones from Sima de los Huesos Middle Pleistocene site (Sierra de Atapuerca, Spain). A phylogenetic approach. *J Hum Evol* 33:283–318.
- Arsuaga JL, et al. (1997) Size variation in Middle Pleistocene Humans. *Science* 277:1086–1088.
- Hublin JJ, Coqueugnot H (2006) Absolute or proportional brain size: That is the question. A reply to Leigh's comments. *J Hum Evol* 50:109–113.
- DeSilva JM, Lesnik JJ (2008) Brain size at birth throughout human evolution: A new method for estimating neonatal brain size in hominins. *J Hum Evol* 55:1064–1074.
- Ponce de León MS, et al. (2008) Neanderthal brain size at birth provides insights into the evolution of human life history. *Proc Natl Acad Sci USA* 105:13764–13768.
- Bermúdez de Castro JM, et al. (2003) Rates of anterior tooth wear in Middle Pleistocene hominins from Sima de los Huesos (Sierra de Atapuerca, Spain). *Proc Natl Acad Sci USA* 100:11992–11996.
- Bermúdez de Castro JM, Martínón-Torres M, Lozano M, Sarmiento S, Muela A (2004) Paleodemography of the Atapuerca-Sima de los Huesos hominin sample: A revision and new approaches to the paleodemography of the European Middle Pleistocene population. *J Anthropol Res* 60:5–26.
- Manzi G, Gracia A, Arsuaga JL (2000) Cranial discrete traits in the Middle Pleistocene humans from Sima de los Huesos (Sierra de Atapuerca, Spain). Does hypostosis represent any increase in “ontogenetic stress” along the Neanderthal lineage? *J Hum Evol* 38:425–446.
- Huang MHS, et al. (1996) The differential diagnosis of posterior plagiocephaly: True lambdoid synostosis versus positional molding. *Plast Reconstr Surg* 98:765–774.
- Cohen MM, Jr, MacLean RE (2000) *Craniosynostosis. Diagnosis, Evaluation and Management*, eds Cohen MM, Jr, MacLean RE (Oxford Univ Press, New York), pp 119–143.
- Smartt JM, Reid R, Singh DJ, Bartlett SP (2007) True lambdoid craniosynostosis: Long-term results of surgical and conservative therapy. *Plast Reconstr Surg* 120:993–1003.
- Mulliken JB, et al. (1999) Analysis of posterior plagiocephaly: Deformational versus synostotic. *Plast Reconstr Surg* 103:371–380.
- Panchal J, Uttchin V (2003) Management of craniosynostosis. *Plast Reconstr Surg* 111:2032–2048.
- Speltz ML, Kapp-Simon KA, Cunningham M, Marsh J, Dawson G (2004) Single-Suture Craniosynostosis: A Review of Neurobehavioral Research and Theory. *J Pediatr Psychol* 29:651–668.
- Cohen MM, Jr (2000) in *Craniosynostosis. Diagnosis, Evaluation and Management*, eds Cohen MM, Jr, MacLean RE (Oxford Univ Press, New York), pp 103–110.
- Cohen MM, Jr (2000) *Craniosynostosis. Diagnosis, Evaluation and Management*, eds Cohen MM, Jr, MacLean RE (Oxford Univ Press, New York), pp 112–118.
- Rekate HL (1998) Occipital plagiocephaly: A critical review of the literature. *J Neurosurg* 89:24–30.
- Sze RW, et al. (2005) MDCT Diagnosis of the child with posterior plagiocephaly. *Am J Rad* 185:1342–1346.
- Ehert FW, Whelan MF, Ellenbogen RG, Cunningham ML, Gruss JS (2004) Differential diagnosis of the trapezoid-shaped head. *Cleft Palate Craniofac J* 41:13–19.
- Kapp-Simon KA, Speltz ML, Cunningham ML, Patel PK, Tomita T (2007) Neurodevelopment of children with single suture craniosynostosis: A review. *Childs Nerv Syst* 23:269–281.
- Kabbani H, Raghuvver TS (2004) Craniosynostosis. *Am Fam Physic* 69:2863–2870.
- Dean V (2004) Effects of different kinds of cranial deformation on the incidence of wormian bones. *Am J Phys Anthropol* 123:146–155.
- Cohen MM, Jr (2000) *Craniosynostosis. Diagnosis, Evaluation and Management*, eds Cohen MM, Jr, MacLean RE (Oxford Univ Press, New York), pp 51–68.
- Mathijssen IM, et al. (1999) Tracing craniosynostosis to its developmental stage through bone center displacement. *J Craniofac Gen Dev Biol* 19:57–63.
- Delashaw JB, Persing JA, Broaddus WC, Jane JA (1989) Cranial vault growth in craniosynostosis. *J Neurosurg* 70:159–165.

37. Higginbottom MC, Jones KL, James HE (1980) Intrauterine constraint and craniosynostosis. *Neurosurgery* 6:39–44.
38. Raco A, et al. (1999) Congenital torticollis in association with craniosynostosis. *Childs Nerv Syst* 15:163–168.
39. Bermejo E, et al. (2005) Craniofacial dysostosis: Description of the First four Spanish Cases and Review. *Am J Med Genet* 41–48.
40. Shahinian HK, et al. (1998) Obstetrical factors governing the etiopathogenesis of lambdoid synostosis. *Am J Perinat* 15:281–286.
41. Pérez PJ, Gracia A, Martínez I, Arsuaga JL (1997) Paleopathological evidence of the cranial remains from the Sima de los Huesos Middle Pleistocene site (Sierra de Atapuerca, Spain). Description and preliminary inferences. *J Hum Evol* 33:409–421.
42. Stuart-Macadam P (1987) A radiographic study of porotic hyperostosis. *Am J Phys Anthropol* 74:511–520.
43. Schultz M (2003) Light microscopic analysis in skeletal paleopathology. *Identification of Pathological Conditions in Human Skeletal Remains*, ed Ortner DJ (Academic, San Diego), pp 73–108.
44. Duggan C, Keener E, Gay B (1970) Secondary Craniosynostosis. *Am J Roentgenol* 19:277–293.
45. Portillo S, Konsol O, Pico P (2004) Cranial Deformity. Importance in General Pediatrics (Translated from Spanish). *Arch Argent Pediatr* 102:190–202.
46. Lordkipanidze D, et al. (2005) The earliest toothless hominin skull. *Nature* 434:717–718.
47. Hublin JJ (1991) Origin of archaic Homo Sapiens: North-West Africa and Western Europe (Translated from French). PhD thesis (University of Bordeaux I), 2 vol.
48. Spoor F, Stringer C, Zonneveld F (1998) Rare temporal bone pathology of the Singa calvaria from Sudan. *Am J Phys Anthropol* 107:41–50.
49. Brothwell DR (1974) in *The Upper Pleistocene Singa Skull: A Problem in Paleontological Interpretation in Bevoelkerungsbiologie*, eds Bernard W, Kandler A (Carl Fisher, Stuttgart), pp 534–545.
50. DeGusta D (2002) Comparative skeletal pathology and the case for congeneric care in Middle Pleistocene hominids. *J Archaeol Sci* 29:1435–1438.
51. Storm RA (2007) *High Prevalence of Premature Craniosynostosis in the Medieval Hospital of St. James and St. Mary Magdalene, Chichester, England*, Seventy-Sixth Annual Meeting of the American Association of Physical Anthropologists, March 28–31, 2007, Philadelphia, PA, p 226.
52. Thompson DNP, Malcolm GP, Jones BM, Harkness WJ, Hayward RD (1995) Intracranial pressure in single-suture craniosynostosis. *Pediatr Neurosurg* 22:235–240.
53. Martínez-Lage JF, Alamo L, Poza M (1999) Raised intracranial pressure in minimal forms of craniosynostosis. *Childs Nerv Syst* 15:11–16.
54. Cinalli G, et al. (1998) Hydrocephalus and Craniosynostosis. *J Neurosurg* 88:209–214.
55. Chaddock WM, Chaddock JB, Boop FA (1992) The subarachnoid spaces in craniosynostosis. *Neurosurgery* 30:867–871.
56. Rasmussen SA, Yazdy MM, Frias JL, Honein MA (2008) Priorities for public health research on craniosynostosis: Summary and recommendations from a centers for disease control and prevention-sponsored meeting. *Am J Med Genet* 146A:149–158.
57. Coussens AK, et al. (2007) Unravelling the molecular control of calvarial suture fusion in children with craniosynostosis. *BioMed Centr Genom* 8:458–482.
58. Becker DB, et al. (2005) Speech, cognitive and behavioral outcomes in nonsyndromic craniosynostosis. *Plast Reconstr Surg* 116:400–407.
59. Arsuaga JL, Martínez I, Gracia A (2001) Phylogenetic Analysis of the Hominids from the Sierra de Atapuerca (Sima de los Huesos and Gran Dolina TD-6): Cranial evidence (Translated from French). *L'Anthropologie* 105:161–178.